DALTON

Kinetics and mechanism of reduction of (*trans*-cyclohexane-1,2-diyldinitrilotetraacetato)manganese(III) by $HONH(SO_3)^-$ and $HON(SO_3)_2^{2-}$†

Frans F. Prinsloo,[a] Jacobus J. Pienaar *[,a] and Rudi van Eldik *[,b]

[a] *Atmospheric Chemistry Research Group, Department of Chemistry, Potchefstoom University, Potchefstoom 2520, South Africa*
[b] *Institute for Inorganic Chemistry, University of Erlangen-Nürnberg, Egerlandstrasse 1, 91058 Erlangen, Germany*

The kinetics and mechanism of the reduction of (*trans*-cyclohexane-1,2-diyldinitrilotetraacetato)manganese(III) by the sulfur–nitrogen oxides $HONH(SO_3)^-$ and $HON(SO_3)_2^{2-}$ in aqueous solution were studied as a function of pH, SN oxide concentration, temperature and pressure. The kinetic data could be interpreted in terms of an inner-sphere electron-transfer mechanism. The two consecutive reaction steps observed at neutral pH were interpreted in terms of rate-determining co-ordination steps that precede the electron-transfer process. Ion chromatographic analyses of the redox products showed that the SN oxides undergo Mn^{III}-catalysed hydrolysis and oxidation reactions. The results are interpreted and discussed in reference to available literature data.

The role of metal-ion-catalysed autoxidation reactions of sulfur(IV) oxides in atmospheric processes have been investigated in detail in recent years.[1–9] These studies clearly demonstrated the important role of redox cycling of the catalytic species, *viz.* Fe^{II}/Fe^{III} and Mn^{II}/Mn^{III} during the overall autoxidation reactions. The oxides of S^{IV}, N^{II} and N^{III} undergo a series of reactions in aqueous solution to produce a range of mixed sulfur–nitrogen (SN) oxides which exhibit a complicated scheme of reactions.[10–14] The chemistry of these species has been studied by a number of groups[13–18] and is well understood. However, only limited information is available on the interaction of SN oxides with metal ions and possible catalysed redox processes. Such processes can have a significant influence on oxidation reactions of the oxides of S^{IV} and $N^{II/III}$.

In previous reports on the metal-catalysed hydrolysis of SN oxides[19–21] we indicated that the presence of these species could significantly affect the oxidation of sulfur(IV) oxides in flue gas desulfurization (FGD) systems used in coal-fired power plants. These studies revealed a rather complicated mechanistic behaviour and the intimate mechanism for the interaction of SN oxides with Mn^{III} remained uncertain mainly due to the instability of such species. In an effort to gain more insight into the mechanism by which Mn^{III} is reduced by SN oxides, we introduced a chelating ligand on the Mn^{III} in order to stabilize the system. For this purpose the complex of manganese(III) with *trans*-cyclohexane-1,2-diyldinitrilotetraacetate (cydta) was selected. It is a strong one-electron oxidant {E_0 = 760 mV for the $[Mn(cydta)]^{-/2-}$ couple[22]} and has for instance been used as a redox partner in studies on the reactivity of the iron–sulfur protein *Chromatium vinosum* HIPIP,[22] H_2O_2,[23] O_2^- and the related enzyme superoxide dismutase,[24] VO^{2+},[25] and $N_2H_5^+$, NH_3OH^+ and a series of benzene-1,2-diols.[26] The reaction of nitrite with this complex has also been used as a possible model for the oxidation of nitrite in biological systems.[27] In the present study we report on the kinetics and mechanism of the electron-transfer reactions between the SN oxides $HONH(SO_3)^-$ and $HON(SO_3)_2^{2-}$ and $[Mn^{III}(cydta)]^-$.

† *Supplementary data available* (No. SUP 57180, 6 pp.): pseudo-first-order rate constants. See Instructions for Authors, *J. Chem. Soc., Dalton Trans.*, 1996, Issue 1.

Experimental

The complex of manganese(III) with cydta was prepared in the crystalline state according to published procedures;[28] cydta was obtained from BDH. Chemical analyses confirmed the purity of the isolated complex‡ {Found: C, 32.8; H, 4.5, N. 6.0. Calc. for $K[Mn(cydta)]\cdot 2.5H_2O$: C, 34.9; H, 4.55; N, 5.8%}. In order to investigate the influence of possible impurities on the rate of the reduction of $[Mn(cydta)]^-$, solutions of it were prepared *in situ* by the electrochemical oxidation of $[Mn^{II}(cydta)]^{2-}$ at a large-surface area platinum anode. Acidic solutions of $[Mn^{III}(cydta)]^-$ are reported to decompose with a rate constant of 6.8×10^{-6} s^{-1} at 25 °C.[28] At pH 7 (10^{-2} mol dm^{-3} phosphate buffer) and $[Mn(cydta)^-] = 2.3 \times 10^{-3}$ mol dm^{-3} (I = 0.1 mol dm^{-3}) a rate constant of 8.6×10^{-5} s^{-1} was reported.[22] All manganese(III) solutions were therefore used within minutes after preparation, in order to reduce the role of spontaneous decomposition reactions. The oxides $HONH(SO_3)^-$ and $HON(SO_3)_2^{2-}$ were synthesized according to literature procedures;[29] $^{\cdot}NO(SO_3)_2^{2-}$ was prepared by electrochemical oxidation of a basic solution of $HON(SO_3)_2^{2-}$. The purity of the SN oxides was checked by ion chromatography. The pH of the test solutions was adjusted to a selected value with a phosphate buffer (0.1 mol dm^{-3}) and measured before and after the reactions. No evidence for the complexation of phosphate with $[Mn(cydta)]^-$ could be detected from UV/VIS spectra of the complex as a function of pH and phosphate concentration. The reference electrode of the pH meter was filled with NaCl (saturated) instead of KCl in order to prevent the precipitation of $KClO_4$, since $NaClO_4$ was used to adjust the ionic strength of the test solutions. Eluents for the ion chromatographic analyses were prepared from sodium carbonate, sodium hydrogencarbonate, tetrabutylammonium hydroxide and acetonitrile. Ion chromatographic analyses were performed on a Waters chromatograph equipped with a HPLC pump and a conductivity detector. Details on the ion chromatographic procedures are given elsewhere.[30]

The UV/VIS spectra were recorded on a Philips PU 8745 spectrophotometer and a Bio Sequential SX-17MV stopped-

‡ Performed at the Department of Chemistry, University of Cape Town, South Africa.

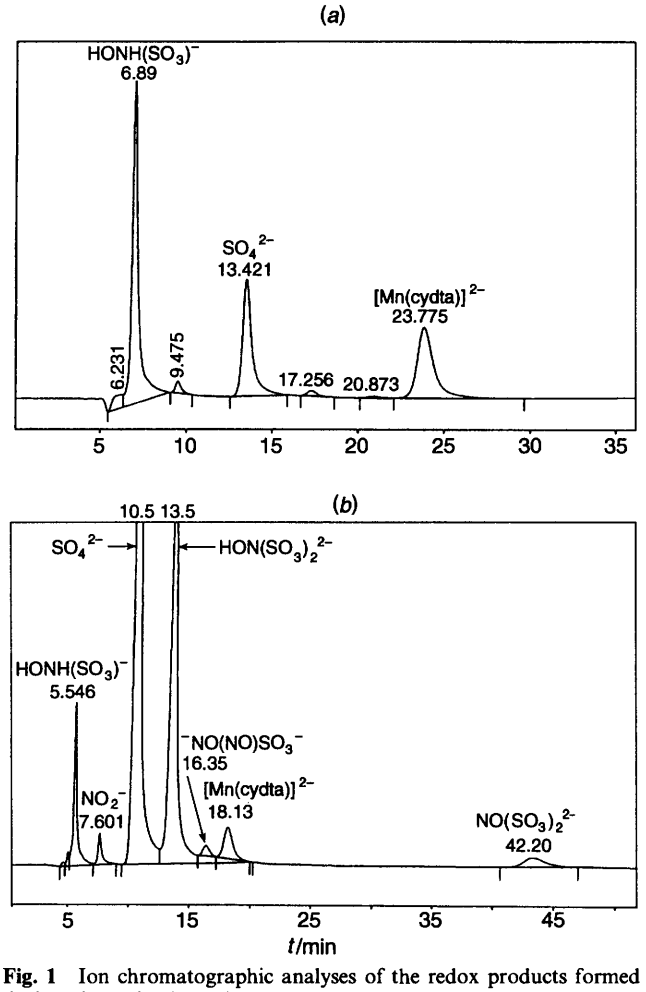

Fig. 1 Ion chromatographic analyses of the redox products formed during the reduction of $[Mn(cydta)]^-$ by (*a*) $HONH(SO_3)^-$ (15% CH_3CN) and (*b*) $HON(SO_3)_2^{2-}$ (20% CH_3CN). Experimental conditions: $[Mn^{III}] = 2 \times 10^{-4}$ mol dm^{-3}, $[SN] = 4 \times 10^{-4}$ mol dm^{-3}

flow spectrofluorimeter. In the latter case time-dependent spectra were generated from individual absorbance *vs.* time traces at different wavelengths. In a typical experiment, repetitive scan spectra were recorded by measuring absorbance changes over a desired time range and at constant wavelength intervals (typically $\Delta\lambda = 10$ nm). In this way multiple-wavelength kinetic data were generated, that are arranged in matrix form with the spectra occupying the rows and the kinetic profiles occupying the columns. Kinetic measurements at ambient pressure were performed on a Bio Sequential SX-17MV stopped-flow spectrofluorimeter which was run on-line with an Applied Photophysics Kinetic Spectrometer Workstation (RISC OS 3 operating system) on which data acquisition and processing was done. Data fitting was performed with the SX.17MV kinetic package. Experiments at elevated pressures (up to 100 MPa) were carried out on a laboratory made high-pressure stopped-flow unit[31] and in this case data fitting was done with the OLIS KINFIT set of programs. All kinetic measurements were performed under pseudo-first-order conditions, *i.e.* an excess of reductant was employed. The reported pseudo-first-order rate constants are the averages from at least 10 kinetic runs.

Results and Discussion

Stoichiometry and products analyses

Analogous to ethylenedinitrilotetracetate (edta),[32] cydta acts as a sexidentate ligand and forms very stable complexes with trivalent metal ions, even more stable than the edta complexes. Stabilities of metal chelates are generally in the order *trans*-cydta > edta > *cis*-cydta. The greater stability of the *trans*-cydta complex of Mn^{III} has been assigned to the rigidity of the cyclohexane ring.[32] In *trans*-cydta the plane of the cyclohexane ring is roughly in the plane of the two nitrogen atoms and the equatorial oxygen atoms from the acetate groups, where it is well away from the rest of the molecule. However, in *cis*-cydta the plane of the cyclohexane ring is oblique to that containing the nitrogen and oxygen atoms, where it interferes with the acetate groups co-ordinated to the metal ion. In the case of chelation with edta, the carbon chain between the nitrogen atoms in the ligand has to be rotated to bring the nitrogen atoms into a favourable position for chelation. In *trans*-cydta there is a restriction on the rotation of the carbon chain, but since the ligand nitrogen atoms are placed very close to each other very little orientation is necessary for chelation to occur. Crystal structure analyses clearly showed these types of complexes to be sexidentate seven-co-ordinate with an approximately pentagonal-bipyramidal structure.[33] In accordance with a literature report,[28] our pH titration curves for the $[Mn(cydta)]^-$ complex with base showed only one deprotonation step at $6 < pH < 11$. A fit of the titration data resulted in a value of $pK_1 = 7.7 \pm 0.2$ at 25 °C and 0.1 mol dm^{-3} ionic strength. No significant deviation in this value was observed when $[Mn(cydta)]^-$ was titrated at different temperatures ($10 < T < 25$ °C). The value of pK_1 is in good agreement with literature values of 8.1[28] and 7.7.[22]

The UV/VIS spectra recorded as function of pH at low $[Mn^{III}]$ are in agreement with literature reports[22,28] and confirm the findings of the titrations. The absorption spectrum of $[Mn(cydta)]^-$ in the range pH 2–6 shows a single absorption maximum at 510 nm with an absorption coefficient of 350 dm^3 mol^{-1} cm^{-1}. At pH $\geqslant 7$ the absorption maximum at 510 nm shifts to 448 nm due to the formation of the hydroxo species with an absorption coefficient of 331 dm^3 mol^{-1} cm^{-1}.

Ion chromatographic analyses of the redox products (see typical examples in Fig. 1) confirmed our earlier findings[20] that Mn^{III} and Fe^{III} catalyse the hydrolysis of SN oxides in a very similar way to the acid-catalysed hydrolysis of these species. When $HON(SO_3)_2^{2-}$ reacts with $[Mn(cydta)]^-$, $^{\bullet}NO(SO_3)_2^{2-}$, $^{-}NO(NO)SO_3^-$ and NO_2^- are formed. It has been reported that $HON(SO_3)_2^{2-}$ is oxidized by Ag_2O to $^{\bullet}NO(SO_3)_2^{2-}$ in alkaline solution[34] and that $^{\bullet}NO(SO_3)_2^{2-}$ decomposes to sulfate, nitrite, $HON(SO_3)_2^{2-}$ and $ON(SO_3)_3^{3-}$.[35] The species $^{-}NO(NO)SO_3^-$ is formed *via* the reaction of nitrite with $HONH(SO_3)^-$[36] which accounts for the low concentration of $HONH(SO_3)^-$ and NO_2^- found during the redox reaction. No $ON(SO_3)_3^{3-}$ could be detected under different conditions $\{2 \times 10^{-4} < [HON(SO_3)_2^{2-}] < 1 \times 10^{-2}$ mol dm^{-3}; $1 \times 10^{-4} < [Mn^{III}] < 1 \times 10^{-3}$ mol dm$^{-3}\}$. If the solution was left standing for a few hours and injected into the ion chromatograph higher concentrations of NO_2^- and no $^{\bullet}NO(SO_3)_2^{2-}$ were found. This further supports the formation of $^{\bullet}NO(SO_3)_2^{2-}$ during the redox reaction and its subsequent decomposition to the products as mentioned above. On the basis of these results the Mn^{III}-catalysed hydrolysis of $HONH(SO_3)^-$ and $HON(SO_3)_2^{2-}$ can be represented by Schemes 1 and 2, respectively, to account for the identified products. Bonding between the Mn^{III} and the nitrogen atom of the SN oxide is suggested to be the initiation step in these schemes. This is analogous to the initiation step in the mechanism proposed for the acid-catalysed hydrolysis of $HON(SO_3)_2^{2-}$,[37a] in which protonation of the amine results in the formation of a reactive complex and subsequent hydrolysis of the SN oxide.

In the reaction sequence outlined in Scheme 2 it is suggested that Mn^{II} is reoxidized to Mn^{III} by $^{\bullet}NO(SO_3)_2^{2-}$. In order to verify this, $[Mn(cydta)]^{3-}$ was mixed with $^{\bullet}NO(SO_3)_2^{2-}$ in excess and the spectral changes monitored. A slow increase in

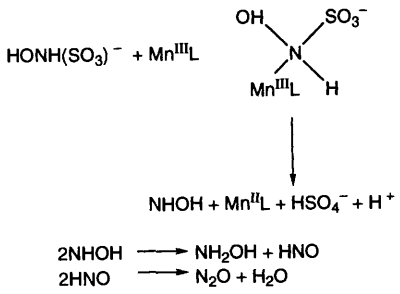

Scheme 1 [see ref. 20(*b*)]. L = cydta

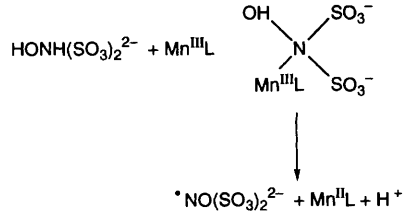

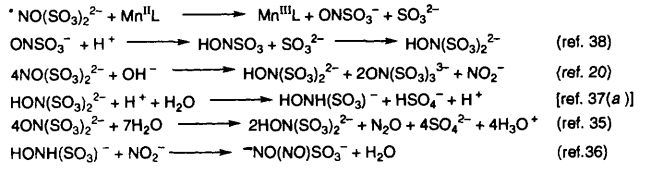

Scheme 2 L = cydta

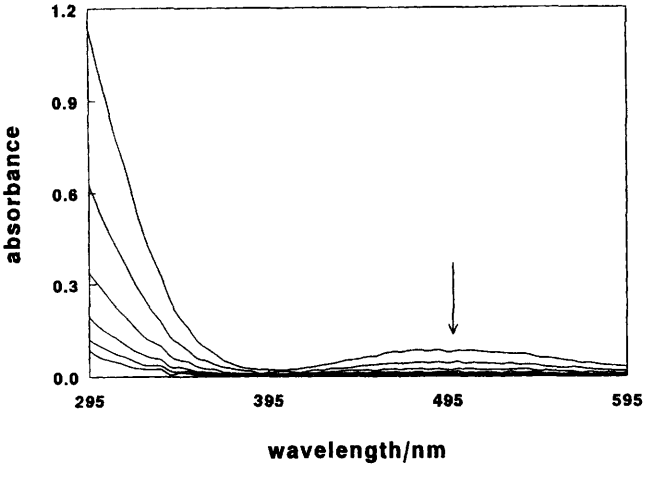

Fig. 2 Rapid-scan spectra illustrating the reduction of $[Mn(cydta)]^-$ by $HONH(SO_3)^-$. Experimental conditions: $[Mn^{III}] = 5 \times 10^{-4}$ mol dm^{-3}, $[HONH(SO_3)^-] = 5 \times 10^{-3}$ mol dm^{-3}; 25 °C, $I = 0.25$ mol dm^{-3}, pH 7; $\Delta t = 0.02$ s

absorbance with a shift in the absorbance maximum to lower wavelength ($\lambda_{max} = 525$ nm) was observed. Ion chromatographic analysis of the reaction mixture showed that $HON(SO_3)_2^{2-}$ is formed during the reaction. This further supports the statement that the reaction between $^{\bullet}NO(SO_3)_2^{2-}$ and [Mn(cydta)] involves a redox process. The product spectrum is a composite of $^{\bullet}NO(SO_3)_2^{2-}$ ($\varepsilon_{radical} = 20.8$ dm^3 mol^{-1} cm^{-1} at $\lambda = 540$ nm [35]) and $[Mn(cydta)]^-$ ($\varepsilon = 350$ dm^3 mol^{-1} cm^{-1} at $\lambda = 510$ nm [28]), as could be verified by starting with the manganese(III) complex.

Kinetic results

The reactions of $[Mn(cydta)]^-$ with the SN oxides $HON(SO_3)_2^{2-}$ and $HONH(SO_3)^-$, $ON(SO_3)_3^{3-}$, $N(SO_3)_3^{3-}$, $HN(SO_3)_2^{2-}$ and $^-NO(NO)SO_3^-$ were studied by monitoring the UV/VIS spectrum of the manganese species and by identifying the redox products by ion chromatography. Contrary to our results [20a] with $[Mn(N_3)]^{2+}$, where all the SN oxides studied reacted, only $HON(SO_3)_2^{2-}$ and $HONH(SO_3)^-$ in this study reacted with $[Mn(cydta)]^-$. This can be attributed to the higher stability of the complex compared to that of $[Mn(N_3)]^{2+}$. The rate of reduction of $[Mn(cydta)]^-$ by $HONH(SO_3)^-$ and $HON(SO_3)_2^{2-}$ was studied by stopped-flow spectrophotometry as a function of pH, [SN oxide], ionic strength, temperature and pressure under pseudo-first-order conditions, *i.e.* at least a ten-fold excess of $HONH(SO_3)^-$ or $HON(SO_3)_2^{2-}$. Measurements were repeated at low and high pH with the electrochemically generated solutions of $[Mn(cydta)]^-$ as a function of $[Mn^{III}]$. In all cases identical results were obtained independent of the source of the manganese(III) complex. The possibility that the reaction involves a photochemical component was ruled out by repeating the same reaction at different slit widths. Identical rate constants were obtained under all conditions.

Typical spectral changes observed when $HONH(SO_3)^-$ reacts with $[Mn(cydta)]^-$ are shown in Fig. 2. The reaction was followed at 500 nm where $[Mn^{III}]$ decreases upon mixing with a SN oxide. Under the selected conditions the acid-catalysed hydrolysis of $HON(SO_3)_2^{2-}$ [37a] and $HONH(SO_3)^-$ [37b] is insignificant and only the redox reaction is observed. The absorbance *vs.* time traces for the reaction of $[Mn(cydta)]^-$ with $HONH(SO_3)^-$ exhibit single exponential functions at pH < 6, but clearly two consecutive exponential functions at pH > 6. In the case of $HON(SO_3)_2^{2-}$ only one exponential function was observed under all conditions. The observed rate constants as a function of all the mentioned parameters are summarized in SUP 57180. A comparison of the observed rate constants for both systems immediately indicated that $HONH(SO_3)^-$ is much more reactive than $HON(SO_3)_2^{2-}$, which is in agreement with our earlier observations.[19,20] In general there is a linear dependence of k_{obs} on the SN oxide concentration, except for the second reaction step for $HONH(SO_3)^-$ at higher pH where a non-linear dependence is observed (see further discussion). The higher reactivity of $HONH(SO_3)^-$ encouraged us to investigate this system in more detail.

For the reaction of $[Mn(cydta)]^-$ with $HONH(SO_3)^-$ both reaction steps exhibit a characteristic pH dependence as shown in Fig. 3. The pH dependence of the slow reaction at pH $\geqslant$ 7 exhibits the same trend as that observed for the fast reaction in this pH range. The fast reaction [Fig. 3(*a*)], however, exhibits a more complicated dependence at pH < 7. For the data at pH $\geqslant$ 7 (both reaction steps) the deprotonation of $[Mn^{III}(cydta)(H_2O)]^-$ species, for which we found $pK_1 = 7.7$, can account for the observed effects in that the hydroxo complex $[Mn^{III}(cydta)(OH)]^{2-}$ is the less reactive species. This is not surprising since the seven-co-ordinate aqua complex is expected to be more labile than the six-co-ordinate hydroxo complex. The decrease and subsequent increase in k_{obs} (fast reaction) with decreasing pH must involve some further protonation/deprotonation that drastically affects the reactivity of the $[Mn^{III}(cydta)(H_2O)]^-$ complex. The UV/VIS spectra in the 400–600 nm range for solutions of the complex at 2 < pH < 6, and pH titration experiments in this study and in the literature [22,28,39] showed no evidence for an acid–base equilibrium in this pH range. Nevertheless, the increase in reactivity at 4 < pH < 6.5 with increasing pH is not so uncommon. Similar effects have been reported for the oxidation of a variety of species by $[Mn^{III}(cydta)(H_2O)]^-$.[22,23,25,26,39–45] A pH profile similar to the one in Fig. 3(*a*) was obtained for the oxidation of Thiobacillus *ferrooxidans rusticyanin* by $[Mn^{III}(cydta)(H_2O)]^-$.[39] In most cases the inflection point at pH < 7 was attributed to acid dissociation of the redox partner. However, in some cases [26,39,46] the origin of this inflection point was uncertain and was attributed either to an inner-sphere mechanism in which the pK_a of the ligand was lowered,[26]

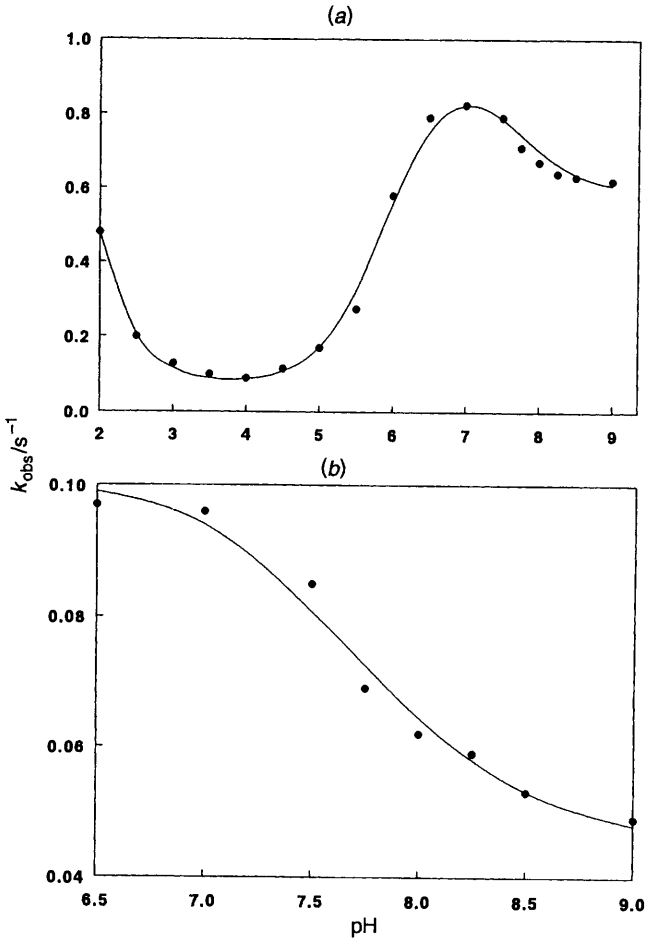

Fig. 3 The pH dependence of k_{obs} for the reduction of $[Mn(cydta)]^-$: (*a*) first reaction step, (*b*) second reaction step. Experimental conditions: $[Mn^{III}] = 5 \times 10^{-4}$ mol dm^{-3}, $[HONH(SO_3)^-] = 5 \times 10^{-3}$ mol dm^{-3}; 25 °C; $I = 0.25$ mol dm^{-3}

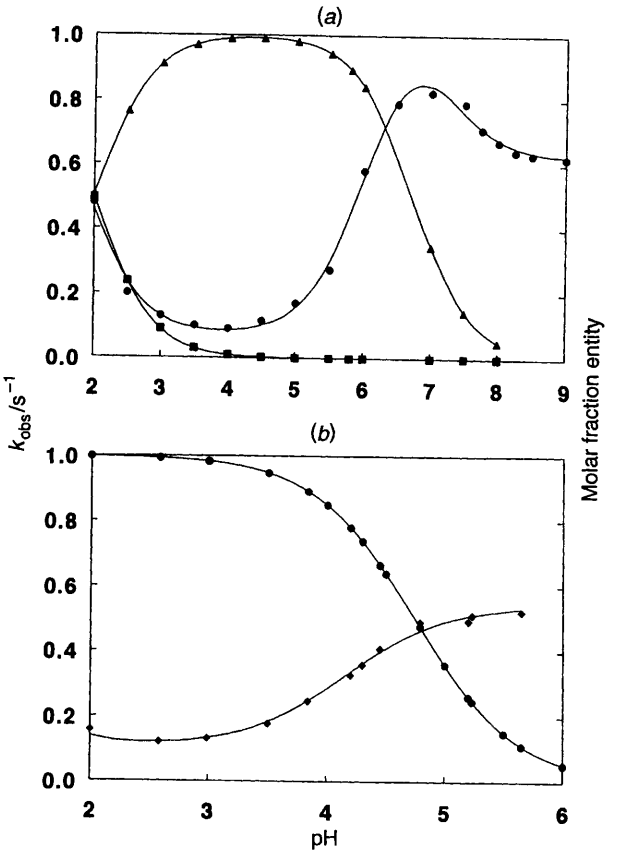

Fig. 4 Distribution curves of (*a*) H_3PO_4 (■) and $H_2PO_4^-$ (▲) and k_{obs} values (●) for the reduction of $[Mn(cydta)]^-$ by $HONH(SO_3)^-$ (first reaction step) and (*b*) $MeCO_2H$ (●) and k_{obs} values (◆) for the reduction of $[Mn(cydta)]^-$ by *T. ferrooxidans* rusticyanin (taken from ref. 39)

or to protonation of one of the carboxylic groups on the cydta ligand.[46] It is also tempting to attribute the increase in reactivity at 4 < pH < 6.5 to a deprotonation process occurring on the $HONH(SO_3)^-$ ligand. However, titrations of $HONH(SO_3)^-$ showed no pK_a in this region or at pH > 6.5 ($K_a = 1.5$ mol dm^{-3} [37b]). A mechanism in which the deprotonation of $HONH(SO_3)^-$ at 4 < pH < 6.5 plays a role can therefore be ruled out. The possibility that the pK_a observed in the range 4 < pH < 6.5 with $[Mn^{III}(cydta)(H_2O)]^-$ is due in part to the protonation of a free carboxylate arm of cydta was discussed previously in the case of the oxidation of rusticyanin from *Thiobacillus ferrooxidans*.[39,46]

It is clear that none of the possibilities outlined here explains the acid dependence at pH < 7. It should be kept in mind though that high concentrations of phosphate buffer were used to stabilize the pH. This high buffer concentration can serve as a source of protons which can *via* general acid catalysis result in protonation of the co-ordinated cydta especially by H_3PO_4 and $H_2PO_4^-$, respectively, in the investigated pH range. Preliminary experiments indicated that the observed rate constants strongly depended on the buffer concentration. This can partly be ascribed to the inability of the buffer to stabilize the pH during the reaction at low buffer concentrations, and partly due to the apparent control over the reactivity of the $[Mn(cydta)]^-$ species as reflected by the buffer-concentration dependence of the observed rate constants. The buffer concentration was therefore selected so high as to obtain rate constants that exhibited no dependence on the buffer concentration. The protonation of the cydta ligand by H_3PO_4 and $H_2PO_4^-$ is suggested to result in its partial dechelation. During the protonation by $H_2PO_4^-$ we suggest that the seven-coordinate $[Mn^{III}(cydta)(H_2O)]^-$ species is converted into a less-reactive pentadentate six-co-ordinate $[Mn^{III}(Hcydta)(H_2O)]$ species. On further protonation by H_3PO_4 the latter species is converted into the more reactive tetradentate six-co-ordinate $[Mn^{III}(H_2cydta)(H_2O)_2]^+$ species. The inclusion of these protonation equilibria can very well account for the observed pH profile in Fig. 3(*a*). The pH profile for the first reaction step, along with the distribution curves for the H_3PO_4 and $H_2PO_4^-$ species, are plotted in Fig. 4(*a*). From this it is clear that the decrease and increase in k_{obs} exactly correspond with the decrease in the H_3PO_4 and increase in the $H_2PO_4^-$ concentrations with increasing pH. In the case of the oxidation of rusticyanin from *Thiobacillus ferrooxidans*, chloroacetic acid (pK_a = 2.85) or sodium acetate buffers (pK_a = 4.75) were used to stabilize the pH between 2.5 and 5.5. It is possible to account for the pH dependence of this redox reaction in the range 2.5 < pH < 6 in a similar way. This is shown in Fig. 4(*b*) where the pH dependence of this reaction is plotted along with the distribution curve for acetic acid, which according to our suggestion is capable of protonating $[Mn^{III}(cydta)(H_2O)]^-$ to form the less-reactive pentadentate six-co-ordinate species at lower pH, *viz.* $[Mn^{III}(Hcydta)(H_2O)]$.

The pH profile for the first reaction step [Fig. 3(*a*)] was therefore interpreted in terms of the reaction sequence outlined in Scheme 3. Using a pre-equilibrium treatment under the assumption that the equilibria in Scheme 3 are rapid, the rate equation (1) can be derived, where $a = [H^+][HPO_4^{2-}] +$

$$k_{obs} = [HONH(SO_3)^-](k_a[H^+][HPO_4^{2-}] + k_bK_1[HPO_4^{2-}] + k_cK_2[H^+][H_2PO_4^-] + k_dK_2K_3[H^+][H_3PO_4])/a \quad (1)$$

$$[Mn^{III}(cydta)(H_2O)]^- \overset{K_1}{\rightleftharpoons} [Mn^{III}(cydta)(OH)]^{2-} + H^+$$

$$[Mn^{III}(cydta)(H_2O)]^- + H_2PO_4^- \overset{K_2}{\rightleftharpoons} [Mn^{III}(Hcydta)(H_2O)] + HPO_4^{2-}$$

$$[Mn^{III}(Hcydta)(H_2O)] + H_3PO_4 \overset{K_3}{\rightleftharpoons} [Mn^{III}(H_2cydta)(H_2O)_2]^+ + H_2PO_4^-$$

$$[Mn^{III}(cydta)(H_2O)]^- + HONH(SO_3)^- \xrightarrow{k_a} \text{products}$$

$$[Mn^{III}(cydta)(OH)]^{2-} + HONH(SO_3)^- \xrightarrow{k_b} \text{products}$$

$$[Mn^{III}(Hcydta)(H_2O)] + HONH(SO_3)^- \xrightarrow{k_c} \text{products}$$

$$[Mn^{III}(H_2cydta)(H_2O)_2]^+ + HONH(SO_3)^- \xrightarrow{k_d} \text{products}$$

Scheme 3

$K_1[HPO_4^{2-}] + K_2[H^+][H_2PO_4^-] + K_2K_3[H^+][H_3PO_4]$. An excellent fit was obtained from a non-linear least-squares fit of the k_{obs} values for the first step as a function of pH using equation (1) [solid line in Fig. 3(*a*)]. To obtain this fit we used literature values for the deprotonation constants for the various phosphate entities at the ionic strength where the measurements were performed ($pK_{H_3PO_4} = 1.991$, $pK_{H_2PO_4} = 6.723$ and $pK_{HPO_4^{2-}} = 11.605$) and the pK_1 value of 7.7 for the $[Mn^{III}(cydta)(H_2O)]^-$ complex from our titration experiments. It turned out that $k_a = 185 \pm 5$ dm^3 mol^{-1} s^{-1}, $k_b = 118 \pm 3$ dm^3 mol^{-1} s^{-1}, $k_c = 15 \pm 3$ dm^3 mol^{-1} s^{-1}, $k_d = (1.6 \pm 0.2) \times 10^3$ dm^3 mol^{-1} s^{-1}, $K_2 = 0.14 \pm 0.02$ and $K_3 = (7.7 \pm 1.1) \times 10^{-3}$. According to these data the reactivity order for the formation of the inner-sphere species in which $HONH(SO_3)^-$ is co-ordinated to Mn^{III} (see Scheme 1) follows the sequence $[Mn^{III}(H_2cydta)(H_2O)_2]^+ > [Mn^{III}(cydta)(H_2O)]^- > [Mn^{III}(cydta)(OH)]^{2-} > [Mn^{III}(Hcydta)(H_2O)]$. It follows that the six-co-ordinate diaqua complex is the most reactive species at low pH (< 4), whereas the seven-co-ordinate aqua complex is the most reactive species in the range 5 < pH < 8. The less-reactive species are the six-co-ordinate aqua (pH 4) and the hydroxo (pH > 8) complexes. The high reactivity of the seven-co-ordinate aqua complex is most probably related to the fact that displacement of co-ordinated water will follow a dissociative mechanism.[6]

The order of reactivity for the different complex species can be compared with that of different aminopolycarboxylatoiron complexes. In this case the redox potentials (*vs.* normal hydrogen electrode, NHE) of $Fe^{III/II}L$ are 0.12 (L = edta, a seven-co-ordinate and approximately pentagonal-bipyramidal structure with one co-ordinated water molecule), 0.16 V [L = carboxymethyliminobis(ethylenenitrilo)tetraacetate (dtpa), a seven-co-ordinate structure with no co-ordinated H_2O molecules], 0.33 [L = nitrilotriacetate (nta), a quadridentate octahedral structure with two co-ordinated water molecules] and 0.77 V (L = H_2O).[47] The following order of reactivity was found when these different iron(II) complexes are oxidized by NO_2^-: hedta > dtpa > edta {hedta = [carboxymethyl)(hydroxyethyl)amino]ethylene nitrilodiacetate, which forms a six-co-ordinate complex with at least one co-ordinated water molecule}.[47] Similarly, it was found that the order of reactivity for the $Fe^{II}L$ reduction of $[Co(NH_3)_5Cl]^{2+}$, $[Co(en)_2(pvp)Cl]^{2+}$ and $[Co(en)_2(py)Cl]^{2+}$ [(pvp = poly(4-vinylpyridine), en = ethane-1,2-diamine, py = pyridine] is $hedta^- > edta^{2-} > Hdtpa > cydta$.[48,49] It is thus expected that the pentadentate $[Mn^{III}(Hcydta)(H_2O)]$ species will have a lower redox potential than the hexadentate $[Mn^{III}(cydta)(H_2O)]^-$ rendering it less reactive than the latter. On the other hand, an increase in the redox potential is expected for the formation of the tetradentate diaqua complex. In general, in the case of inner-sphere electron-transfer mechanisms, the Mn–OH path usually makes a significant contribution to the overall rate, whereas the aqua complexes predominate in outer-sphere reactions with little or no contribution from the M–OH paths.[50] The above values for the rate constants in equation (1) therefore follow the trend expected for an inner-sphere mechanism.

$$[Mn^{III}(cydta)(H_2O)]^- \overset{K_1}{\rightleftharpoons} [Mn^{III}(cydta)(OH)]^{2-} + H^+$$

$$[Mn^{III}(cydta)(OH)]^{2-} + [Mn^{III}(cydta)(H_2O)]^- \overset{K_4}{\rightleftharpoons} [(cydta)Mn(\mu\text{-}O)Mn(cydta)]^{4-} + H_2O + H^+$$

$$[(cydta)Mn(\mu\text{-}O)Mn(cydta)]^{4-} + HONH(SO_3)^- \xrightarrow{k_a'} \text{products (pH} > 6)$$

Scheme 4

It should be mentioned that various models were developed and tested in order to explain the pH profile in Fig. 3(*a*). In one such model it was postulated that $H_2PO_4^-$ could react with the $[Mn^{III}(cydta)(H_2O)]^-$ complex to form a less-reactive species in which it is co-ordinated in some way. In this case the decrease and increase in k_{obs} exactly correspond with the increase and decrease in the $H_2PO_4^-$ concentration with increasing pH [see Fig. 4(*a*)], which suggests that $H_2PO_4^-$ interacts with $[Mn^{III}(cydta)(H_2O)]^-$ in such a way that a less-reactive species is produced. Although this model apparently fitted the data rather well, it was not possible to obtain realistic values for either the deprotonation constant for $H_2PO_4^-$ or for the rate constant for the reaction of the less-reactive species with $HONH(SO_3)^-$.

The pH profile for the second reaction step [Fig. 3(*b*)] can be interpreted in terms of the dimeric complex that is produced in the reactions outlined in Scheme 4. On dissociation this complex forms the labile aqua or less-reactive hydroxo complex that can rapidly undergo substitution by $HONH(SO_3)^-$, followed by the electron-transfer step. It has previously been illustrated that Fe^{III}(edta) complexes dimerize at relatively high $[Fe^{III}]$ and high pH, where each unit of the dimer adopts a quinquedentate six-co-ordinate geometry in the solid state and in aqueous solution.[6] In our case, at relatively high $[Mn^{III}]$ and at moderately high pH values, precipitates are formed which are probably due to the formation of similar dimeric species. In accordance with the Fe^{III}(edta) system, it is therefore possible that a μ-O bridged complex can be formed as suggested in Scheme 4. The pH profile for this reaction step is very similar to that for the first reaction step at pH > 6, which suggests the reactive species is a hydroxo- or oxo-bridged complex in which protonation leads to formation of the more-reactive species. For this hypothesis to be valid the second step should not be observed at lower $[Mn^{III}]$. This was indeed the case and supports the explanation for the second step. The pH profile for the second reaction step [Fig. 3(*b*)] can therefore be explained by the reaction sequence outlined in Scheme 4. It represents an increase in the concentration of the dimeric species with increasing $[Mn^{III}]$. This means that the bridged complex is more stable and therefore less reactive than the monomeric aqua species, which could be related to the way in which the cydta is co-ordinated to the Mn^{III}.[33]

Detailed kinetic measurements, including a study of the $[HONH(SO_3)^-]$, temperature and pressure dependence, were undertaken for the first reaction step at pH 4 and 7, *i.e.* at the minimum and maximum rate where mainly $[Mn^{III}(Hcydta)(H_2O)]$ and $[Mn^{III}(cydta)(H_2O)]^-$ are present in solution, respectively. The $[HONH(SO_3)^-]$ concentration dependence of k_{obs} [Fig. 5(*a*)] is linear and exhibits a small intercept at higher temperatures. The latter can be related to a slow spontaneous decomposition reaction of $[Mn(cydta)]^-$ at pH 4, which does not occur to a significant extent at lower temperature or at higher pH. The data for pH 7 [Fig. 5(*b*)] clearly underline this statement, the dependence on

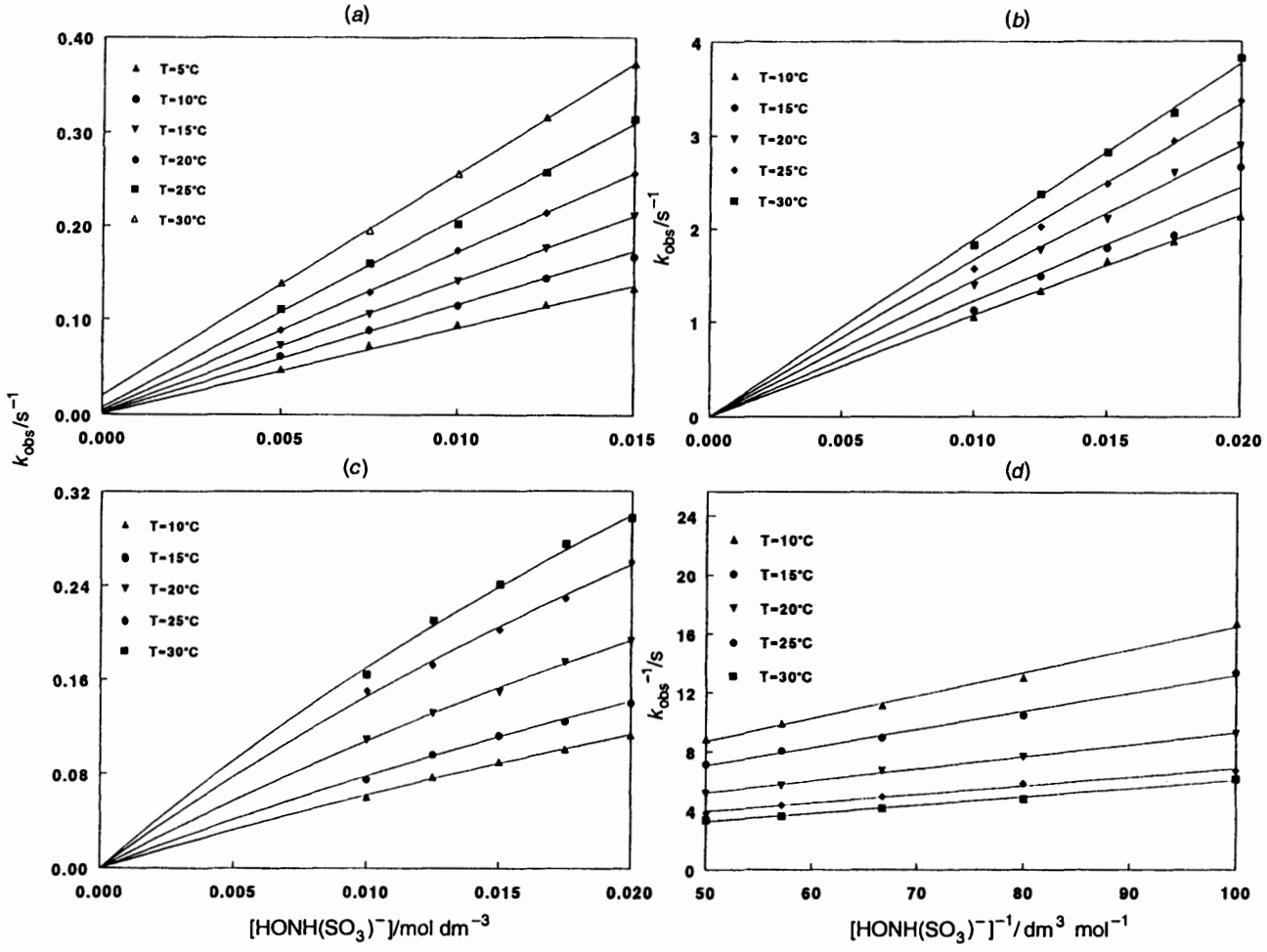

Fig. 5 Plots of k_{obs} *versus* $[HONH(SO_3)^-]$: temperature dependence for (*a*) the first step at pH 4, (*b*) the first step at (pH 7) and (*c*) the second step (at pH 7). In (*d*) are shown plots of $1/k_{obs}$ *versus* $1/[HONH(SO_3)^-]$ for the reduction of $[Mn(cydta)]^-$ at pH 7 (second step). Experimental conditions: $[Mn^{III}] = (0.5–1) \times 10^{-3}$ mol dm^{-3}; $I = 0.25$ mol dm^{-3}

$$Mn^{III}L + HONH(SO_3)^- \overset{K}{\rightleftharpoons} \{Mn^{III}L{\cdot}HONH(SO_3)^-\}$$
$$\downarrow k$$
$$[Mn^{III}L\{N(OH)H(SO_3)\}]^-$$
$$\downarrow \text{fast}$$
$$\text{products}$$

Scheme 5 L = cydta

$$[LMn(\mu\text{-}O)MnL]^{4-} + HONH(SO_3)^- \overset{K'}{\rightleftharpoons}$$
$$\{LMn(\mu\text{-}O)MnL^{4-}{\cdot}HONH(SO_3)^-\}$$
$$\downarrow k'$$
$$[LMn(\mu\text{-}O)MnL\{N(OH)H(SO_3)\}]^{5-}$$
$$\downarrow \text{fast}$$
$$\text{products}$$

Scheme 6 L = cydta

$[HONH(SO_3)^-]$ being linear with no significant intercept. The concentration dependence is ascribed to a complex-formation reaction (see Scheme 1), the details of which in terms of an interchange mechanism are given in Scheme 5. The formation of $[Mn^{III}L\{N(OH)H(SO_3)\}]^-$ is followed by a rapid intramolecular electron-transfer reaction to produce NHOH, Mn^{II} and HSO_4^- (Scheme 1). The rate equation for this process is given in (2), which simplifies to $k_{obs} = kK[HONH(SO_3)^-]$ in the

$$k_{obs} = kK[HONH(SO_3)^-]/\{1 + K[HONH(SO_3)^-]\} \quad (2)$$

absence of any curvature in plots of k_{obs} *versus* $[HONH(SO_3)^-]$. The values of kK as a function of temperature are summarized in Table 1.

For the slow reaction observed at pH 7 the $[HONH(SO_3)^-]$ dependence is not linear and exhibits significant curvature [see Fig. 5(*c*)]. This is ascribed to stronger precursor formation in the case of the less-reactive dimeric species, followed by the formation of an inner-sphere species that undergoes a rapid electron-transfer process as outlined in Scheme 6.

The data in Fig. 5(*c*) can be fitted with equation (3), and the

$$k_{obs} = k'K'[HONH(SO_3)^-]/\{1 + K'[HONH(SO_3)^-]\} \quad (3)$$

values of k' and K' were calculated from either the double inverse plots [see Fig. 5(*d*)] or from a non-linear least-squares fit routine [solid lines in Fig. 5(*c*)]. Both procedures resulted in similar values for k' and K', summarized as a function of temperature in Table 1. The values of k' are significantly lower than usually found for outer-sphere reactions of $[Mn(cydta)]^-$,[24] indicating that such a process is not the rate-determining step. The values for K' are very similar to those obtained for other inner-sphere reactions,[48] which further supports the suggestion that reduction by $HONH(SO_3)^-$ proceeds according

Table 1 Rate constants and activation parameters for the reactions of $HONH(SO_3)^-$ and $HON(SO_3)_2^{2-}$ with $[Mn(cydta)]^-$ [a]

pH	SN	T/°C	p/MPa	$[Mn^{III}]$/ mol dm^{-3}	Step	kK/dm^3 mol^{-1} s^{-1}	k'/s^{-1}	K'/dm^3 mol^{-1}	$k'K'$/dm^3 mol^{-1} s^{-1}
4	$HONH(SO_3)^-$	5	*b*	5×10^{-4}	1	10.6 ± 0.5			
		10			1	12.9 ± 0.3			
		15			1	14.1 ± 0.1			
		20			1	17.2 ± 0.1			
		25			1	20.8 ± 0.2			
	$\Delta H^{\ddagger}$/kJ mol^{-1}					22 ± 1			
	$\Delta S^{\ddagger}$/J K^{-1} mol^{-1}					−147 ± 5			
		30			1	25.4 ± 0.3			
4		25	5	5×10^{-4}	1	19.0 ± 0.3			
			25		1	21.2 ± 0.3			
			50		1	24.4 ± 0.5			
			75		1	26.1 ± 0.4			
			100		1	28.2 ± 0.3			
	$\Delta V^{\ddagger}$/cm^3 mol^{-1}					−10 ± 1			
7		10	*b*	1×10^{-3}	1	107 ± 1			
					2		0.68 ± 0.18	10.0 ± 3.1	6.81 ± 0.30
		15			1	121 ± 5			
					2		0.75 ± 0.20	11.6 ± 3.6	8.70 ± 0.44
		20			1	144 ± 2			
					2		0.93 ± 0.18	13.1 ± 3.1	12.2 ± 0.5
		25			1	166 ± 2			
					2		1.14 ± 0.27	14.6 ± 4.3	16.6 ± 1.0
		30			1	188 ± 2			
					2		1.24 ± 0.32	15.9 ± 5.1	18.1 ± 1.3
	$\Delta H^{\ddagger}$/kJ mol^{-1}					18 ± 1	21 ± 2		
	$\Delta S^{\ddagger}$/J K^{-1} mol^{-1}					−142 ± 2	−175 ± 7		
7	$HON(SO_3)_2^{2-}$	25	*b*	(0.5–1) × 10^3		25.1 ± 0.3			

[a] Experimental conditions: I = 0.25 mol dm^{-3}, reactions followed at 500 nm. [b] Atmospheric.

to an inner-sphere mechanism. The thermal activation and thermodynamic parameters were calculated in the usual way, and are also included in Table 1.

The pressure dependence of this reaction was studied at pH 4 (see Table 1), where the reaction is insensitive to a possible shift in pH associated with a change in pressure. The values of kK increase significantly with increasing pressure, which corresponds to a $\Delta V^{\ddagger}$ value of -10 ± 1 cm^3 mol^{-1}. The latter is in agreement with the significantly negative $\Delta S^{\ddagger}$ value, indicating that the formation of the $[Mn^{III}L\{HONH(SO_3)\}]$ species is characterized by a highly ordered transition state. Under the conditions selected (pH 4), $[Mn^{III}(Hcydta)(H_2O)]$ is the main species in solution, which can undergo an associative-interchange substitution mechanism since it is suggested to be a pentadentate six-co-ordinate species. According to the $\Delta S^{\ddagger}$ value at pH 7 for the first reaction step, a similar mechanism must be operative for the $[Mn^{III}(cydta)(H_2O)]^-$ complex. The latter is suggested to be a sexidentate seven-co-ordinate complex, and the co-ordinated water molecule is expected to be significantly more labile than in the case of the $[Mn^{III}(Hcydta)(H_2O)]$ complex. Thus a changeover from I_a to I_d on increasing the pH from 4 to 7 cannot be ruled out. In this case the negative $\Delta S^{\ddagger}$ value for kK at pH 7 can partly be due to the contribution of the precursor complex-formation step. The activation parameters for the second step at pH 7 also suggest the complex formation with $HONH(SO_3)^-$ to have a strongly associative nature, as can be seen from the very negative $\Delta S^{\ddagger}$ value for k'.

The results of this study demonstrated that not only is the hydrolysis of $HONH(SO_3)^-$ and $HON(SO_3)_2^{2-}$ catalysed by $[Mn(cydta)]^-$, $HON(SO_3)_2^{2-}$ is also oxidized by this complex. The non-reactivity of the other SN oxides is rather unexpected, but the reactivity pattern for $HONH(SO_3)^-$ and $HON(SO_3)_2^{2-}$ is consistent with reported data.[20] In general the kinetic data point to an inner-sphere electron-transfer mechanism for the reduction of $[Mn(cydta)]^-$ by the investigated SN oxides. This is in accordance with reports on the corresponding reduction by other organic and inorganic compounds.[23,25,26,39,41–43,51] To our knowledge the activation volume for the oxidation of $HONH(SO_3)^-$ at pH 4 is the first such value reported for reactions in which $[Mn(cydta)]^-$ is the oxidizing agent. It confirms in general that this type of redox reaction proceeds according to an inner-sphere electron-transfer mechanism. An outer-sphere electron-transfer mechanism has been proposed only in a few cases for this complex as the redox partner.[52,53] Furthermore little information is available on reactions in which SN oxides react with metal ions or complexes and the mechanistic details reported in this study are therefore unique. The indirect interference of the buffer species with the redox processes was clearly observed in this study. The majority of reactions in which $[Mn(cydta)]^-$ was the oxidizing agent were performed in the presence of buffers, and it is therefore likely that also in these cases the buffer species could have interfered with the investigated redox reactions.

Acknowledgements

The authors gratefully acknowledge financial support from the Foundation for Research Development (SA), ESKOM Technology Research and Investigations, the Deutsche Forschungsgemeinschaft and the Ministerium für Forschung und Technologie.

References

1 J. Kraft and R. van Eldik, *Inorg. Chem.*, 1989, **28**, 2297, 2306.
2 J. Kraft and R. van Eldik, *Atmos. Environ.*, 1989, **23**, 2709.
3 K. Bal Reddy, N. Coichev and R. van Eldik, *J. Chem. Soc., Chem. Commun.*, 1991, 481.
4 K. Bal Reddy and R. van Eldik, *Atmos. Environ.*, 1992, **26A**, 661.
5 N. Coichev and R. van Eldik, *Inorg. Chim. Acta*, 1991, **185**, 69.
6 M. Dellert-Ritter and R. van Eldik, *J. Chem. Soc., Dalton Trans.*, 1992, 1037, 1045.
7 N. Coichev and R. van Eldik, *New J. Chem.*, 1994, **18**, 123.
8 J. Berglund, S. Fronaeus and L. I. Elding, *Inorg. Chem.*, 1993, **32**, 4527.
9 J. Ziajka, F. Beer and P. Warneck, *Atmos. Environ.*, 1994, **28**, 2549.

10 W. Pasuik-Bronikowska and K. J. Rudzinski, *Chem. Eng. Commun.*, 1982, **18**, 287.
11 S. G. Chang, D. Littlejohn and N. H. Lin, *ACS Symp. Ser.*, 1982, **188**, 127.
12 D. Littlejohn and S. G. Chang, *Environ. Sci. Techol.*, 1984, **18**, 305.
13 D. Littlejohn and S. G. Chang, *Anal. Chem.*, 1986, **58**, 158.
14 D. Littlejohn, K. J. Hu and S. G. Chang, *Inorg. Chem.*, 1986, **25**, 3131.
15 D. Littlejohn and S. G. Chang, *Energy Fuels*, 1991, **5**, 249.
16 T. K. Ellison and C. A. Eckert, *J. Phys. Chem.*, 1984, **88**, 2335.
17 L. R. Martin, D. E. Damschen and H. S. Judeikis, *Atmos. Environ.*, 1981, **15**, 191.
18 E. Sada, H. Kumazawa and H. Hikosaka, *Ind. Eng. Chem., Fundam.*, 1984, **23**, 60: 1986, **25**, 386; *Ind. Eng. Chem. Res.*, 1987, **26**, 2016.
19 H. Gutberlet, B. Pätch, R. van Eldik and F. F. Prinsloo, Power Plant Chemistry 1993, VGB Conference, Essen, 1993.
20 (*a*) F. F. Prinsloo, J. J. Pienaar, R. van Eldik and H. Gutberlet, *J. Chem. Soc., Dalton Trans.*, 1994, 2373; (*b*) V. Lepentsiotis, F. F. Prinsloo, R. van Eldik and H. Gutberlet, *J. Chem. Soc., Dalton Trans.*, 1996, 2135.
21 F. F. Prinsloo, J. J. Pienaar and R. van Eldik, *J. Chem. Soc., Dalton Trans.*, 1995, 293.
22 I. K. Adzamli, D. M. Davies, C. S. Stanley and A. G. Sykes, *J. Am. Chem. Soc.*, 1981, **103**, 5543.
23 T. E. Jones and R. E. Hamm, *Inorg. Chem.*, 1974, **13**, 1940.
24 Z. Bradic and R. G. Williams, *J. Am. Chem. Soc.*, 1984, **106**, 2236.
25 D. J. Boone, R. E. Hamm and J. P. Hunt, *Inorg. Chem.*, 1972, **11**, 1060.
26 P. Arselli and E. Mentasti, *J. Chem. Soc., Dalton Trans.*, 1983, 689.
27 T. E. Jones and R. E. Hamm, *Inorg. Chem.*, 1975, **14**, 1027.
28 R. E. Hamm and M. A. Suwyn, *Inorg. Chem.*, 1967, **6**, 139.
29 G. K. Rollefson and C. F. Oldershaw, *J. Am. Chem. Soc.*, 1932, **54**, 977; E. Degener and F. Seel, *Z. Anorg. Allg. Chem*, 1956, **285**, 129.
30 M. Geissler and R. van Eldik, *Anal. Chem.*, 1992, **64**, 3004.
31 R. van Eldik, W. Gaede, S. Wieland, J. Kraft, M. Spitzer and D. A. Palmer, *Rev. Sci. Instrum.*, 1993, **64**, 1355.
32 R. J. Day and C. N. Reilly, *Anal. Chem.*, 1965, **37**, 1326.
33 S. Richards, B. Pedersen, J. V. Silverton and J. L. Hoard, *Inorg. Chem.*, 1964, **3**, 27; G. H. Cohen and J. L. Hoard, *J. Am. Chem. Soc.*, 1966, **88**, 3228.
34 T. Haga, *J. Chem. Soc.*, 1904, 78.
35 J. H. Murib and D. M. Ritter, *J. Am. Chem. Soc.*, 1952, **74**, 3394.
36 S. B. Oblath, S. S. Markowitz, T. Novakov and S. G. Chang, *Inorg. Chem.*, 1983, **22**, 579.
37 (*a*) S. Naiditch and D. M. Yost, *J. Am. Chem. Soc.*, 1941, **63**, 2123; (*b*) D. Littlejohn, A. Wizansky and S. G. Chang, *Can. J. Chem.*, 1989, **67**, 1596.
38 P. N. Balasubramanian and E. S. Gould, *Inorg. Chem.*, 1983, **22**, 1100.
39 J. McGinnis, W. J. Ingledew and A. G. Sykes, *Inorg. Chem.*, 1986, **25**, 3730.
40 S. Gangopadhya, M. Ali, S. K. Saha and P. Banerjee, *J. Chem. Soc., Dalton Trans.*, 1991, 2729.
41 S. Gangopadhya, M. Ali and P. Banerjee, *J. Chem. Soc., Perkin Trans. 2*, 1992, 781.
42 S. Gangopadhya, M. Ali and P. Banerjee, *Bull. Chem. Soc. Jpn.*, 1992, **65**, 517.
43 S. Gangopadhya, M. Ali, A. Dutta and P. Banerjee, *J. Chem. Soc., Dalton Trans.*, 1994, 841.
44 T. Satyanarayana and N. R. Anipindi, *Transition Met. Chem.*, 1992, **17**, 325.
45 S. Gangopadhya, S. K. Saha and P. Banerjee, *Transition Met. Chem.*, 1991, **16**, 355.
46 J. McGinnis, J. D. Sinclair and A. G. Sykes, in *Biochemical and Inorganic Aspects of Copper Coordination Chemistry*, eds. K. D. Karlin and J. Zubieta, Adenine Press, Guilderland, NY, 1986.
47 V. Zang and R. van Eldik, *Inorg. Chem.*, 1990, **29**, 4462 and refs. therein.
48 Y. Kurimura, *Bull. Chem. Soc. Jpn.*, 1973, **46**, 2093.
49 Y. Kurimura, I. Sekine, E. Tsuchida and Y. Karino, *Bull. Chem. Soc. Jpn.*, 1974, **47**, 1823.
50 R. Banerjee, R. Das and A. K. Chakraburtty, *J. Chem. Soc., Dalton Trans.*, 1991, 987 and refs. therein.
51 S. Gangopadhya, S. K. Saha, M. Ali and P. Banerjee, *Int. J. Chem. Kinet.*, 1991, **23**, 105.
52 R. N. Mehrotra and R. G. Wilkins, *Inorg. Chem.*, 1980, **19**, 2177.
53 D. H. Macartney and D. W. Thompson, *Inorg. Chem.*, 1989, **28**, 2195.

Received 23*rd May* 1996; *Paper* 6/03596E